Inorg. Chem. **2008**, *47*, 690–698

Lead and Aluminum Bonding in Pb–Al Metaphosphate Glasses

J. E. Tsuchida,[†] J. Schneider,*[,†] P. S. Pizani,[‡] and S. L. Oliveira[†]

Instituto de Física de São Carlos, Universidade de São Paulo, Av. Trabalhador São-Carlense 400, Centro CEP 13566-590, CP369 São Carlos-SP, Brazil, and Departamento de Física, UFSCAR, Rodovia Washington Luiz, Km 235, CP 676, CEP 13565-905, São Carlos, SP, Brazil

Received August 30, 2007

The bonding properties of cations in phosphate glasses determine many short- and medium-range structural features in the glass network, hence influencing bulk properties. In this work, Pb–Al–metaphosphate glasses $(1 - x)Pb(PO_3)_2 \cdot xAl(PO_3)_3$ with $0 \leq x \leq 1$ were analyzed to determine the effect of the substitution of Pb by Al on the glass structure in the metaphosphate composition. The glass transition temperature and density were measured as a function of the Al concentration. The vibrational and structural properties were probed by Raman spectroscopy and nuclear magnetic resonance of ^{31}P, ^{27}Al, and ^{207}Pb. Aluminum incorporates homogeneously in the glass creating a stiffer and less packed network. The average coordination number for Al decreases from 5.9 to 5.0 as x increases from 0.1 to 1, indicating more covalent Al–O bonds. The coordination number of Pb in these glasses is greater than 8, showing an increasing ionic behavior for compositions richer in Al. A quantitative analysis of the phosphate speciation shows definite trends in the bonding of AlO_n groups and phosphate tetrahedra. In glasses with $x < 0.48$, phosphate groups share preferentially only one nonbridging O corner with an AlO_n coordination polyhedron. For $x > 0.48$ more than one nonbridging O can be linked to AlO_n polyhedra. There is no corner sharing of O between AlO_n and PbO_n polyhedra nor between AlO_n themselves throughout the compositional range. The PbO_n coordination polyhedra show considerable nonbridging O sharing, with each O participating in the coordination sphere of at least two Pb. The bonding preferences determined for Al are consistent with the behavior observed in Na–Al and Ca–Al metaphosphates, indicating this may be a general behavior for ternary phosphate glasses.

Introduction

Phosphate glasses have particular properties such as low glass transition (T_g) and dilatometric softening temperatures, high thermal expansion coefficients (TEC), and high UV transparency. Some of these properties make them suitable materials for applications in low-temperature sealing,[1−3] in laser host matrices (doped with rare-earth ions),[4,5] and even in the confinement of nuclear wastes.[6,7] The low chemical durability of phosphate glasses can be substantially improved by the addition of chemical species, notoriously by aluminum.[8,9] Lead is another interesting species that can be incorporated in binary phosphate glasses up to proportions as large as 60 mol %.[10] Though lead metaphosphate has low chemical resistance to leaching, Pb may preserve the low-T_g and high-TEC values of ternary phosphate glasses, due to its relatively high ionic field strength and ion polarizability.

The glass network in phosphates is composed of a backbone of PO_4 tetrahedra, which can be classified according to their mutual connectivity using the notation Q^n, where n is the number of bridging oxygen atoms (BO) shared with other n tetrahedra. The basic P_2O_5 network, composed of Q^3 groups, may be depolymerized by the addition of a modifier oxide, creating nonbridging oxygens (NBO) cor-

* To whom correspondence should be addressed. E-mail: schnei@if.sc.usp.br.
[†] Universidade de São Paulo.
[‡] UFSCAR.

(1) Peng, Y. B.; Day, D. E. *Glass Technol.* **1991**, *32* (6), 166−173.
(2) He, Y.; Day, D. E. *Glass Technol.* **1992**, *33* (6), 214−219.
(3) Donald, I. W. *J. Mater. Sci.* **1993**, *11*, 2841−2886.
(4) Jiang, S.; Myers, M.; Peyghambarian, N. *J. Non-Cryst. Solids* **1998**, *239*, 143−148.
(5) Dai, S.; Sugiyama, A.; Hu, L.; Liu, Z.; Huang G.; Jiang, Z. *J. Non-Cryst. Solids* **2002**, *311*, 138−144.
(6) Donald, I. W.; Metcalfe, B. L.; Taylor, R. N. J. *J. Mater. Sci.* **1997**, *32*, 5851−5887.
(7) Donald, I. W.; Metcalfe B. L. *J. Non-Cryst. Solids* **2004**, *348*, 118−122.
(8) Brow, R. *J. Am. Ceram. Soc.* **1993**, *76* (4), 913−918.
(9) Brow, R.; Kirkpatrick, R. J.; Turner, G. L. *J. Am. Ceram. Soc.* **1993**, *76* (4), 919−928.
(10) Lockyer, M. W. G.; Holland, D.; Howes, A. P.; Dupree, R. *Solid State Nucl. Magn. Reson.* **1995**, *5*, 23−34.

10.1021/ic701707a CCC: $40.75
Published on Web 12/15/2007

responding to Q^2, Q^1, and Q^0 groups, appearing as the concentration of the modifier increases.[11] Metal cations (Me) coordinate these NBO, defining some degree of short range organization according to the strength of the Me−O bond. The comprehension of the correlation between the bonding properties of the cation and the short-/medium-range structure is crucial to understand the behavior of many properties of phosphate glasses. For example, in Na−Al phosphate glasses the behavior of density, T_g, and TEC as a function of composition can be explained in terms of the hardening of the network through the formation of P−O−Al linkages at the expense of weaker P−O−Na linkages.[8,9]

In phosphate glasses, Al shows an intermediate character between network modifier and former, respectively evidenced by assuming 6-fold or 4-fold coordination, depending on the composition of the system.[8−10] The more covalent Al−O bonds associated with low-coordinated Al create a mixed alumino−phosphate network with direct effect on the glass properties. Lead also shows an intermediate character. For example, in silicate glasses lead behaves as an intermediate element depending on the composition, assuming coordination numbers (CN_{Pb}) around 4.[12−14] In contrast, lead in phosphate glasses seems to play a modifier role. Values of CN_{Pb} from 5 up to 12 were determined with different techniques in glasses and crystals.[15−18] For example, crystalline lead metaphosphate, $Pb(PO_3)_2$, has two crystallographic sites for Pb with coordinations 7 and 8.[19] In the $Pb(PO_3)_2$ glass, values of $CN_{Pb} = 8 \pm 1$ were determined through EXAFS and XANES techniques[15] and $CN_{Pb} = 8.8 \pm 0.7$ through X-ray diffraction.[16]

Several studies have shown the connection between the cation bonding properties, as valence and coordination number, and the short and intermediate order of binary glasses near ultraphosphate compositions.[20,21] Compositional anomalies observed in density and T_g of several binary phosphates were explained according to these models.[21,22] One fundamental factor is the relation between the coordination number of the cation (CN_{Me}) and the ratio of terminal O per P-tetrahedron (M_{TO}), which are the O atoms interacting strongly with the modifier Me cation. For glasses with $M_{TO} > CN_{Me}$, the preferred structural arrangement in the glass, involves linkages through terminal O between PO_4 tetrahedra and dispersed MeO_n groups, thus forming a corner-sharing network of coordination polyhedra. As the concentration of oxide is increased, for compositions with $M_{TO} < CN_{Me}$ the MeO_n polyhedra are forced to share corners, edges, and possibly faces.[20] Such a systematic description is still lacking in ternary phosphates, due to the structural complexities introduced by the presence of two chemical species. However, results obtained in Na−Al and Ca−Al metaphosphates indicate that some of these short- and medium-range bonding preferences are also applicable to describe the structural evolution of ternary glasses with composition.[23,24] These observations brought up the possibility to extend these concepts and methods to ternary phosphates. The simplification of the phosphate backbone topology is a necessary condition in ternary systems to deal with the structural complexities and analyze the effects associated specifically to the cation properties. The meta composition ([O/P] = 3) is an advantageous option, because the phosphate network will be composed mainly by long chains or cycles of tetrahedra. In addition, the possibility of establishing structure/bond correlations in ternary phosphates requires a systematic analysis as a function of the ratio between both cation species and also with consideration of species with different properties, such as valence and Me−O bond strength.

A previous structural study carried on Pb−Al phosphate glasses focused on the network repolymerization by Al[10] for compositions with different [O/P] ratios. In the present work, we studied systematically the structural effects caused by the cation substitution for a fixed [O/P] ratio. A series of Pb−Al−metaphosphate glasses $(1 - x)Pb(PO_3)_2 \cdot xAl(PO_3)_3$ with molar fraction in the range $0 \leq x \leq 1$ was analyzed using nuclear magnetic resonance (NMR) of ^{31}P, ^{27}Al, and ^{207}Pb and Raman spectroscopy. The distribution of phosphates species and the coordination environments of Al and Pb were studied as a function of the Al concentration. Glass transition temperatures and densities were measured as a function of the composition. The evolution of the phosphate speciation was described quantitatively in terms of simple models considering the bonding properties of Al with the phosphate network, providing a general picture of the connectivity between PbO_n and AlO_n polyhedra with PO_4 tetrahedra. The behavior of the coordination number for Pb was analyzed, providing information of the connectivity regime between PbO_n polyhedra.

Experimental Procedure

Glasses with composition $(1 - x)Pb(PO_3)_2 \cdot xAl(PO_3)_3$ were prepared by the conventional melt quenching method. The $Pb(PO_3)_2$ compound was prepared from reagent grade PbO and $NH_4H_2PO_4$ as starting materials. Commercial reagent grade $Al(PO_3)_3$ powder was used. The metaphosphate powders were mixed at the desired proportions and melted in Zn−Al−Si crucibles at temperatures between 1100 and 1600 °C in air and poured on brass molds previously heated. Annealing treatments were performed on each sample for 4 h at 25 °C below their respective T_g. The chemical composition of the samples was analyzed using an energy dispersive

(11) Van Wazer, J. R. *Phosphorus and Its Compounds*; Interscience: New York, 1958; Vol. 1.
(12) Wang P.; Zahng, L. *J. Non-Cryst. Solids* **1996**, *194*, 129−134.
(13) Fayon, F.; Bessada, C.; Massiot, D.; Farnan Coutures, J. P. *J. Non-Cryst. Solids* **1998**, *403*, 232−234.
(14) Hoppe, U.; Kranold, R.; Ghosh, A.; Landron, C.; Neuefeind Jóvári, P. *J. Non-Cryst. Solids* **2003**, *328*, 146−156.
(15) Greaves, G. N.; Gurman, S. J.; Gladden, L. F.; Spence, C. A.; Cox, P.; Sales, B. C.; Boatner, L. A.; Jenkins, R. N. *Philos. Mag.* **1988**, *B58*, 271−283.
(16) Musinu, A.; Paschina, G.; Piccaluga, G.; Pinna, G. *J. Non-Cryst. Solids* **1994**, *177*, 97−102.
(17) Fayon, F.; Farnan, I.; Bessada, C.; Coutures, J.; Massiot, D.; Coutures, J. P. *J. Am. Chem. Soc.* **1997**, *119*, 6837−6843.
(18) Muñoz, F.; Agulló-Rueda, F.; Montagne, L.; Marchand, R.; Durán, A.; Pascual, L. *J. Non-Cryst. Solids* **2004**, *347*, 153−158.
(19) Jost, K. H. *Acta Cryst.* **1964**, *17*, 1539−1544.
(20) Hoppe, U. *J. Non-Cryst. Solids* **1996**, *195*, 138−147.
(21) Brow, R. *J. Non-Cryst. Solids* **2000**, *263&264* (1−4), 1−28.
(22) Brow, R.; Click C.; Alam, T. *J. Non-Cryst. Solids* **2000**, *274*, 9−16.
(23) Schneider, J.; Oliveira, S. L.; Nunes L. A. O.; Panepucci, H. *J. Am. Ceram. Soc.* **2003**, *86*, 317−324.
(24) Schneider, J.; Oliveira, S. L.; Nunes, L. A. O.; Bonk, F. *Inorg. Chem.* **2005**, *44*, 423−430.

Table 1. Analyzed Composition for Pb−Al Metaphosphate Glasses

$Al(PO_3)_3$ (molar fractn)	PbO (mol %)	Al_2O_3 (mol %)	P_2O_5 (mol %)	$Al(PO_3)_3$ (molar fractn)	PbO (mol %)	Al_2O_3 (mol %)	P_2O_5 (mol %)
0	55	0	45	0.48	25	16	59
0.03	46	3	51	0.58	19	20	61
0.08	45	4	51	0.61	21	19	60
0.12	43	5	52	0.73	13	23	64
0.15	42	8	50	0.80	9	25	66
0.22	37	8	55	0.85	7	26	67
0.25	36	8	56	0.89	5	27	68
0.28	34	11	55	0.94	3	28	69
0.38	30	11	59	1	0	28	72

X-ray spectrometer (LEO 440-EDX Oxford detector), giving the results shown in Table 1. The glassy state of the samples was confirmed from X-ray diffraction experiments. Densities of the glasses at room temperature were measured through the Archimedes method using ethylene glycol as immersion liquid, with an uncertainty within ± 0.05 g/cm^3. The T_g of the glasses was determined from differential scanning calorimetry (DSC) performed in a TA Instruments DSC-2910 calorimeter, under N_2 atmosphere in platinum crucibles with a heating rate of 10 °C min^{-1}. The uncertainty on the temperatures was estimated as ± 3 °C.

Raman spectra were obtained with a Jobin-Yvon T6400 micro-Raman spectrometer with triple monochromator, using as excitation source an Ar−Kr laser Coherent-Innova 70C Spectrum operating at 488 nm.

High-resolution magic angle spinning (MAS) NMR spectra were obtained at magnetic field of 9.4 T in a spectrometer Varian Unity INOVA. Measurements were carried out under MAS of up to 12 kHz in 4 mm silicon nitride rotors. The ^{31}P NMR spectra were obtained from single pulse experiments with $\pi/2$ pulses of 3 μs length and recycle delays of 800 s. For ^{27}Al NMR, the pulse duration was 0.5 μs ($\pi/16$) and recycle delays were 5 s. Triple quantum-MAS ^{27}Al NMR experiments (3Q-MAS) were carried out to measure the ^{27}Al isotropic chemical shift, δ_{iso}, and the quadrupole coupling constant $P_q = e^2qQ/h(1 + \eta^2/3)^{1/2}$. Here eq and η are respectively the principal value and the asymmetry parameter of the electric field gradient tensor at the position of the nucleus, and eQ is the quadrupole moment of the nucleus. The pulse sequence used for 3Q-MAS has two pulses for generation−reconversion of 3Q coherences into observable ones,[25] with durations of 6 and 2 μs, respectively, and intensity of 120 kHz. An additional Z-filter selective pulse of 10 μs length and 5 kHz strength was also applied.[26] Typically, 256 hypercomplex FID signals were collected with 2048 points each, 1 s recycle delay, and up to 2048 scans in the glasses with the lowest Al concentration. ^{207}Pb NMR spectra were measured in static conditions at the same magnetic field in a wide-line 7 mm probe, using a Hahn spin−echo sequence with $\pi/2$ pulse of 4 μs length and pulse separation of 60 μs. To improve the signal-to-noise ratio, the whole spin−echo signal was acquired and properly phased. The variable off-set cumulative spectroscopy technique (VOCS) was applied to obtain the broad ^{207}Pb spectrum of each sample.[27] Up to six different experiments with 60 kHz step in irradiation frequency were performed to cover the whole spectral range, 1 s of recycle delay, and a number of scans between 12 000 and 35 000. References for ^{31}P and ^{27}Al chemical shifts were 85% H_3PO_4 and 0.1 M $Al_2(SO_4)_3$ solutions, respectively. For ^{207}Pb, a solid lead nitrate sample was used as secondary standard, with δ_{iso} of −3494 ppm with respect to tetramethyllead.

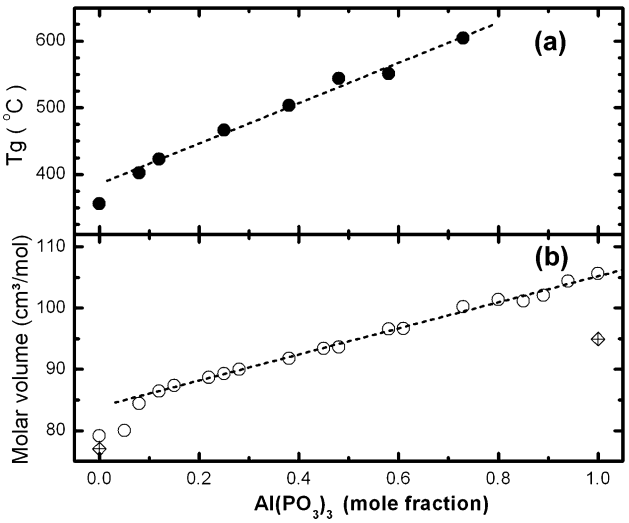

Figure 1. (a) Glass transition temperature and (b) molar volume for the glasses $(1 - x)Pb(PO_3)_2 \cdot xAl(PO_3)_3$: squares, molar volume for the crystals $Pb(PO_3)_2$ ($x = 0$) and $Al(PO_3)_3$ ($x = 1$); straight lines, linear least-square fittings.

Results

DSC and Molar Volume. Figure 1a shows the variation of the glass transition temperature T_g as a function of the concentration of Al in the glasses, up to the highest temperatures supported by the DSC instrument. There is a linear increase of T_g for concentrations above 0.1 mol of $Al(PO_3)_3$. This behavior arises from a uniform substitution of Pb by Al atoms establishing stronger, more covalent, bonds with NBO. Cross-linking of phosphate chains through Al−O−Al bridges restricts the mobility these groups, increasing the T_g of the glass.

The molar volume, V_m, of the glasses was determined from the measurement of the densities. Figure 1b shows the behavior of V_m with the composition, which is also linear for concentrations above 0.1 mol of $Al(PO_3)_3$. As in the case of T_g, the linearity indicates uniform replacement of cation species. The increase in V_m indicates that the substitution of Pb by Al creates a more open glass network. For the extreme compositions, the difference of V_m between $Pb(PO_3)_2$ in glass and crystal samples is about 2%, while for $Al(PO_3)_3$ the difference is 11%. The latter case indicates substantial differences between the glass and crystal structures. For glasses below 0.1 mol of $Al(PO_3)_3$, there are noticeable deviations with respect to the linear trend observed for V_m at higher concentrations. In these Pb-rich glasses, the more compact packing shows that the arrangement of the phosphate backbone should be qualitatively different from the other compositions. Such difference may be also related to the slightly lower T_g value for the $Pb(PO_3)_2$ glass. More compact packing and lower T_g may indicate that many Pb−O bonds are established with NBO of the same phosphate chain and many PbO_n coordination polyhedra share edges or faces among them, as observed in the $Pb(PO_3)_2$ crystal.[19]

Raman Spectroscopy. Figure 2 shows the Raman spectra for the series of glasses and for the crystals $Pb(PO_3)_2$ and

(25) Medek, A.; Harwood, J. S.; Frydman, L. *J. Am. Chem. Soc.* **1995**, *117*, 12779−12787.
(26) Amoreaux, J.-P.; Fernandez, C.; Steuernagel, S. *J. Magn. Reson., A* **1996**, *123*, 116−118.
(27) Massiot, D.; Farnan, I.; Gauthier, N.; Trumeau, D.; Trokiner, A.; Coutures, J. P. *Solid State NMR* **1995**, *4*, 241−248.

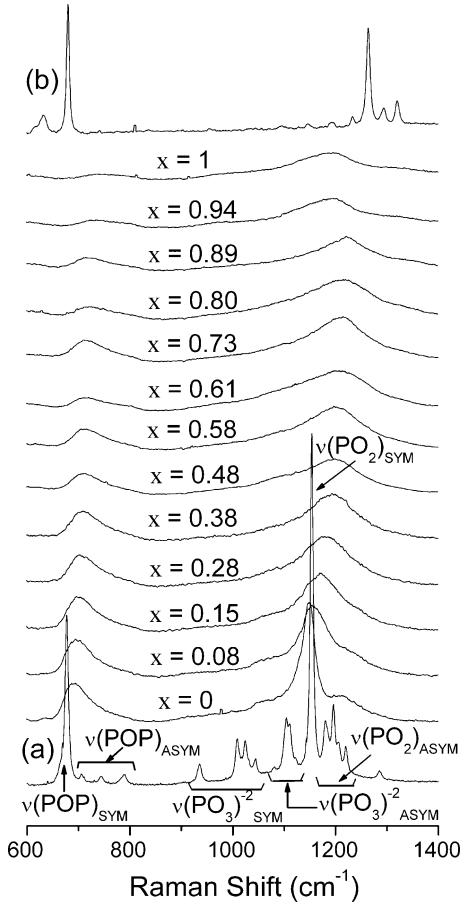

Figure 2. Raman spectra for the glasses $(1 - x)Pb(PO_3)_2 \cdot xAl(PO_3)_3$ and the crystalline compounds (a) $Pb(PO_3)_2$ and (b) $Al(PO_3)_3$: SYM, symmetric vibrations; ASYM, asymmetric vibrations.

$Al(PO_3)_3$. The bands in the wavelength region between 600 and 1400 cm^{-1} were identified according to literature data for phosphate glasses and crystalline lead phosphates.[28−31] The Raman spectrum for crystalline $Pb(PO_3)_2$ (Figure 2a) shows bands from six vibrational modes. The bands with the highest wavenumbers correspond to the stretching vibrations involving the NBO from Q^2 phosphates. The most intense peak corresponds to symmetric mode $\nu(PO_2)_{SYM}$ around 1155 cm^{-1}. The asymmetric stretching $\nu(PO_2)_{ASYM}$ is located around 1195 cm^{-1}. The second most intense band, around 680 cm^{-1}, was attributed to the symmetric stretching $\nu(POP)_{SYM}$ of BO in Q^2 groups. The bands between 710 and 790 cm^{-1} correspond to the asymmetric stretching $\nu(POP)_{ASYM}$ of the same groups. The frequency region between 930 and 1125 cm^{-1} corresponds to stretching vibrations from BO in Q^1 units, the symmetric modes $\nu(PO_3)_{SYM}$ around 1025 cm^{-1}, and the asymmetric $\nu(PO_3)_{ASYM}$ around 1110 cm^{-1}. The trace with $x = 0$ in Figure 2 corresponds to the spectrum of the $Pb(PO_3)_2$ glass, which shows broadened bands keeping a good correlation with those identified in the crystal. As Al is introduced in the glass, the same set of Raman bands can still be recognized. The stretching vibrations from Q^2 phosphates appear in the range 690−800 cm^{-1} for BO and 1150−1250 cm^{-1} for NBO, with the symmetric and asymmetric modes, respectively, in the low- and high-wavenumber ends of each region. There is a systematic increase in the Raman shift as the Al concentration is increased. The effect is more pronounced for the NBO stretching modes, reflecting the direct interaction of these oxygens with the Al cations. As O−Al bonds are less ionic than O−Pb, the frequency of these vibrations should increase. Also, the substitution of Pb atoms by Al reduces the effective masses of the modes, contributing also to the increase in frequencies. As seen in Figure 2, these frequencies take intermediate values between those observed in the crystals, resembling the case of the solid-solution behavior in mixed crystals.[32] For compositions up to $x = 0.9$, the frequencies for $\nu(POP)_{SYM}$ and $\nu(PO_2)_{SYM}$ increase uniformly, indicating a homogeneous bonding of Pb and Al to the NBO atoms in the glass. However, for glasses with $x = 0.94$ and $x = 1$, the frequencies of the $\nu(PO_2)$ bands decrease. This effect may be related to a specific local rearrangement in the network with respect to glasses with lower Al concentration. In the case of the $\nu(POP)$ vibrations, the frequencies in the $Al(PO_3)_3$ crystal are lower than in glasses with high Al content, by about 70 cm^{-1} for $x = 1$. This substantial hardening of the $\nu(POP)$ modes in the glasses may indicate more strained P−O−P bridges within the phosphate chains with respect to the crystal.

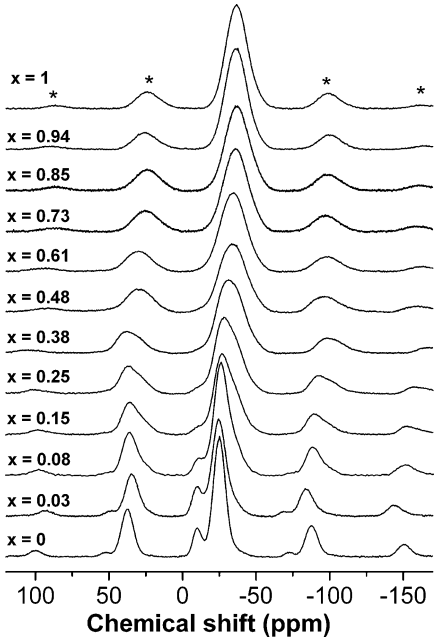

Figure 3. ^{31}P MAS NMR spectra for the glasses $(1 - x)Pb(PO_3)_2 \cdot xAl(PO_3)_3$. Asterisks indicate spinning sidebands.

NMR Spectroscopy. ^{31}P NMR. Figure 3 shows the ^{31}P NMR spectra for the set of glasses. For compositions with low x, three resonance lines can be identified in the spectra, centered at −10, −25, and −36 pmm (shoulder). The first two lines, observed in the $Pb(PO_3)_2$ glass, can be attributed

(28) Dayanand, C.; Bhikshamaiah, G.; Tyagaraju, V. J.; Salagram, M.; Murthy, A. S. R. K. *J. Mater. Sci.* **1996**, *8*, 1945−1967.
(29) Hudgens, J. J.; Brow, R. K.; Tallant D. R.; Martin, S. W. *J. Non-Cryst. Solids* **1998**, *223*, 21−31.
(30) Efimov, A. M. *J. Non-Cryst. Solids* **1997**, *209*, 209−226.
(31) Le Saout, G.; Simon, P.; Fayon, F.; Blin, A.; Vaills, Y. *J. Raman Spectrosc.* **2002**, *33*, 740−746.
(32) Chang, I. F.; Mitra, S. S. *Adv. Phys.* **1971**, *20*, 359−404.

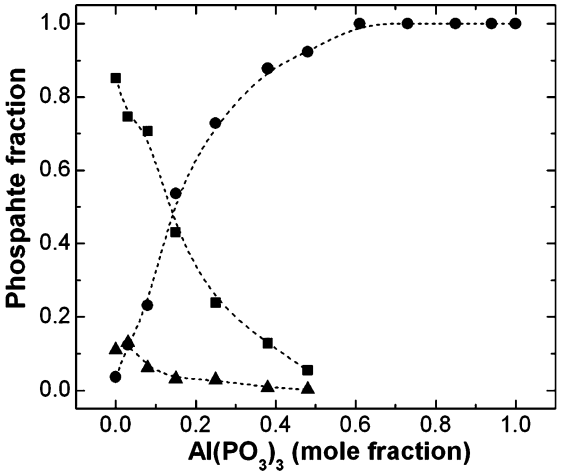

Figure 4. Fraction of Q^n species as a function of the composition for the glasses $(1 - x)Pb(PO_3)_2 \cdot xAl(PO_3)_3$: triangles, Q^1; squares, Q^2; circles, $Q^2(m\text{Al})$ ($m = 1, 2$). Lines are for guidance purpose only.

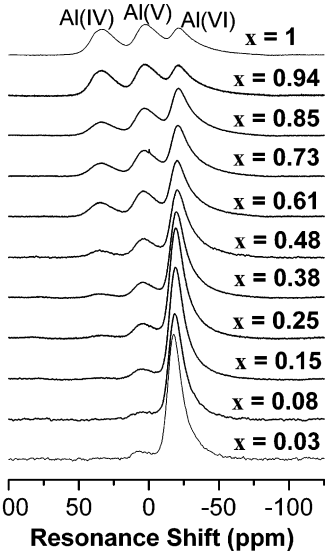

Figure 5. ^{27}Al MAS NMR spectra for the glasses $(1 - x)Pb(PO_3)_2 \cdot xAl(PO_3)_3$.

to Q^1 and Q^2 units. The shoulder at approximately −36 ppm may be associated with Q^3 units. As observed in a previous study on binary lead phosphates, the Q^n populations in the $Pb(PO_3)_2$ glass have some degree of disproportion, according to the pseudoreaction $2Q^2 \leftrightarrow Q^1 + Q^3$.[33] By introduction of Al to this system, the low frequency shoulder grows in intensity. This increase cannot be attributed to more Q^3 units, and more disproportion, because the Q^1 resonance becomes progressively weaker. Therefore, the increase of the signal intensity on the low frequency shoulder may indicate new nonequivalent Q^2 species. According to the literature, each NBO linked to Al produces a low-frequency shift between 7 and 10 ppm on Q^2 resonances,[9,34] which is compatible with the position of the observed shoulder. These species will be identified here as $Q^2(m\text{Al})$, where $m = 1$ or 2 is the number of NBO atoms coordinated by Al in the Q^2 tetrahedron. For glasses with low Al concentration, the strongest ^{31}P NMR line corresponds to Q^2 tetrahedra with both NBO atoms coordinated by Pb. As will be discussed later, in these glasses of low Al concentration the low frequency shoulder may be attributed mainly to $Q^2(1\text{Al})$ species, i.e., having only one NBO coordinated by Al. As more Al is incorporated into the base $Pb(PO_3)_2$ glass, the Q^1 resonance becomes progressively weaker and the intensity of the $Q^2(m\text{Al})$ shoulder increases. For compositions above $x = 0.48$, the Q^1 line disappears and it is not possible to resolve individual Q^2 or $Q^2(m\text{Al})$ lines. The spectrum remains broad and quite symmetric up to the composition with $x = 1$. To quantify the phosphate speciation, Gaussian functions representing individual Q^n resonances were fitted to the ^{31}P NMR spectra. The intensities of each central line and its sidebands were considered in this quantification. Figure 4 shows the resulting fractions of Q^n species as a function of composition, following the variations described above. As will be shown

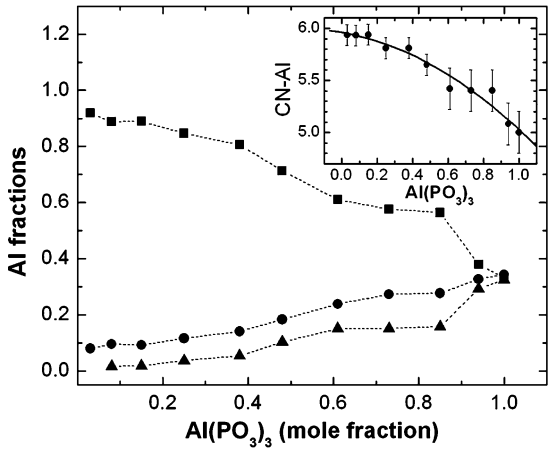

Figure 6. Fraction of Al in coordinations IV (triangles), V (circles), and VI (squares) in the glasses $(1 - x)Pb(PO_3)_2 \cdot xAl(PO_3)_3$. Inset: Mean coordination number for Al calculated from the fractional populations. Lines are for guidance purposes only.

later, the analysis of the evolution of Q^n populations may yield valuable information about the glass structure of this system.

^{27}Al NMR. Figure 5 shows the ^{27}Al NMR spectra for the set of glasses. The observed peaks centered about 33.5, 2.5, and −22 ppm are related to Al in coordination IV−VI, respectively. Figure 6 shows the relative fraction of Al in these coordination environments, obtained from the fitting of quadrupolar powder patterns to each line, using the values of δ_{iso} and P_q measured in the ^{27}Al-3Q-MAS experiments described below. The inset in Figure 6 shows the average coordination number CN_{Al} calculated from the fractions of Al in each coordination. In the glasses with high Al content, a substantial amount of Al is in coordination IV, hence demonstrating that this species is also acting as network former in this system. For the $Al(PO_3)_3$ glass, Al is equally distributed among the three coordination environments ($CN_{Al} = 5.0$), revealing a fundamental difference with respect to the crystal, whose structure has Al only in 6-fold coordina-

(33) Fayon, F; Bessada, C; Coutures, J. P.; Massiot, D. *Inorg. Chem.* **1999**, *38*, 5212−5218.
(34) Dollase, W.; Merwin, L.; Sebald, A. *J. Solid State Chem.* **1989**, *83*, 140−49.

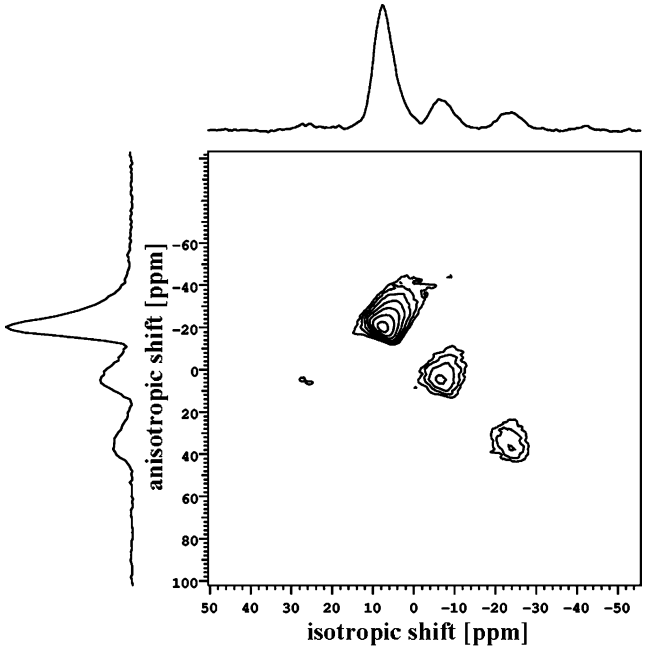

Figure 7. Typical ^{27}Al-3Q-MAS spectrum measured for the set of $(1 - x)Pb(PO_3)_2 \cdot xAl(PO_3)_3$ glasses, corresponding to the glass with $x = 0.73$, showing the signals from ^{27}Al in coordinations IV−VI: horizontal projection, isotropic dimension; vertical projection, anisotropic dimension.

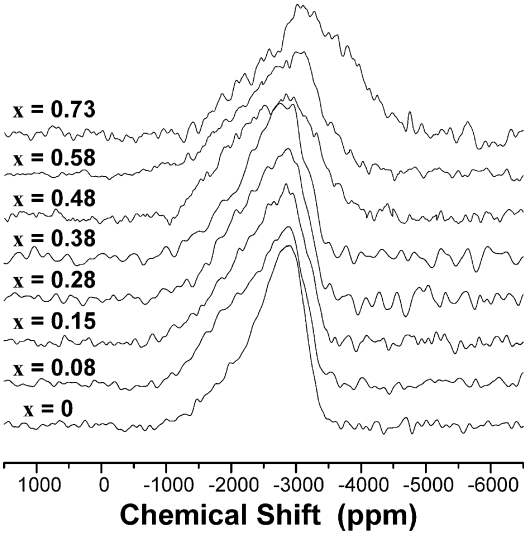

Figure 8. ^{207}Pb NMR static spectra for the glasses $(1 - x)Pb(PO_3)_2 \cdot xAl(PO_3)_3$.

tion.[35] The values for CN_{Al} obtained in the Pb−Al system are higher than those observed in Ca−Al metaphosphate and lower than those in Na−Al metaphosphate.[23,24] This behavior is consistent with the relation between the ionic field strength of these species: 0.35 for Ca^{+2}; 0.27 for Pb^{2+}; 0.17 for Na^{+}.[36] As observed in other phosphates glasses,[37] cations with more intense field establish less ionic bonds with the NBO and require more charge transfer from the neighboring Al^{3+} ions to the phosphates, causing a decrease in the average coordination of Al.

To determine the values of δ_{iso} and P_q for each Al site, ^{27}Al-3Q-MAS experiments were carried out in all the glasses of the set. A typical ^{27}Al-3Q-MAS spectrum is represented in Figure 7, corresponding to the sample with $x = 0.73$, showing the signals from ^{27}Al in the three coordination environments. Table 2 shows the resulting parameters calculated for the observed lines. The values of δ_{iso} for Al(VI) and Al(V) sites show a uniform decrease with the Al content. This behavior is compatible with a homogeneous dispersion of these sites in the glass matrix, without any drastic change in the local structure around Al. The increase in the magnetic shielding with the concentration of Al is expected, as the substitution of a Pb−O by a stronger Al−O bond requires more charge transfer from the phosphate group.[37] This transfer decreases the electronic density around Al nuclei in neighboring Al−O−P bonds, causing a slightly more negative chemical shift. For Al(IV) sites this effect is not observable, probably due to the stronger covalent character of the Al−O bonds. Table 2 also shows the values measured for the quadrupolar coupling parameter P_q. The smaller values correspond to Al(VI), which is in agreement with the higher local symmetry of these sites. The P_q values for Al(VI) sites are slightly higher for glasses with the higher concentration of Al, possibly indicating more strained environments. For the other sites, no clear trends can be inferred within the uncertainty of the values.

^{207}Pb NMR. Figure 8 shows the ^{207}Pb NMR spectra measured with the VOCS technique for glasses with compositions up to $x = 0.73$. In glasses with lower Pb concentration, the signal-to-noise ratio was too low to obtain reliable results. The spectra are far too broadened to resolve chemical shift anisotropy patterns from individual atomic environments. In a comparison of these spectra with data from the literature, the observed span of chemical shift indicates ionic Pb−O bonding with coordination number

Table 2. ^{27}Al Isotropic Chemical Shift δ_{iso} and Electric Quadrupole Coupling P_q Measured for Each Al Site in the Glasses, Obtained from ^{27}Al-3Q-MAS Experiments

	δ_{iso} (ppm)			P_q (MHz)		
x	Al(IV)	Al(V)	Al(VI)	Al(IV)	Al(V)	Al(VI)
0.08			−14.5 ± 0.2			0.8 ± 0.5
0.15		12.3 ± 0.2	−14.6 ± 0.2		1.5 ± 0.5	0.9 ± 0.5
0.25		11.9 ± 0.2	−15.1 ± 0.2		1.9 ± 0.5	0.8 ± 0.5
0.38		10.9 ± 0.2	−15.3 ± 0.2		1.7 ± 0.5	0.4 ± 0.5
0.48	41.4 ± 0.2	9.6 ± 0.2	−15.9 ± 0.2	2.0 ± 0.5	1.4 ± 0.5	0.4 ± 0.5
0.61	41.4 ± 0.2	10.0 ± 0.2	−15.6 ± 0.2	2.1 ± 0.5	2.2 ± 0.5	0.9 ± 0.5
0.73	40.4 ± 0.2	9.3 ± 0.2	−16.0 ± 0.2	1.3 ± 0.5	1.1 ± 0.5	0.4 ± 0.5
0.85	39.9 ± 0.2	9.8 ± 0.2	−16.3 ± 0.2	2.0 ± 0.5	1.7 ± 0.5	0.9 ± 0.5
0.94	42.0 ± 0.2	10.9 ± 0.2	−16.2 ± 0.2	2.4 ± 0.5	2.2 ± 0.5	1.4 ± 0.5
1	42.0 ± 0.2	10.6 ± 0.2	−16.3 ± 0.2	2.2 ± 0.5	1.9 ± 0.5	1.3 ± 0.5

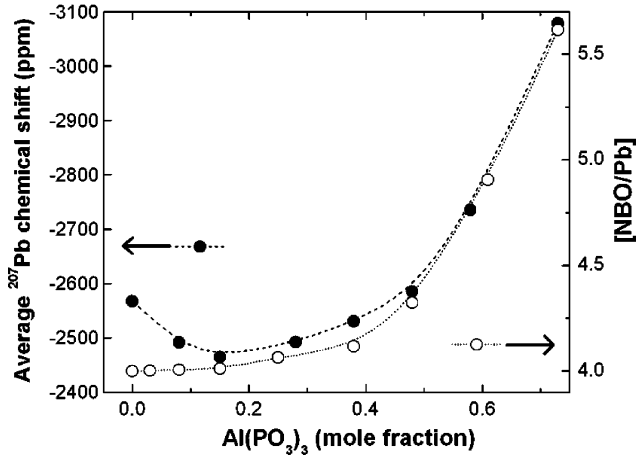

Figure 9. Filled circles: Average ^{207}Pb chemical shift calculated from ^{207}Pb NMR spectra. Blank circles: Ratio [NBO/Pb] calculated from eq 8 using Al-coordination number calculated from ^{27}Al NMR spectra. Lines are for guidance purpose only.

$CN_{Pb} > 7$.[17] The average ^{207}Pb chemical shift obtained from these spectra is plotted in Figure 9, showing a displacement to lower frequencies as the concentration of Pb is decreased, i.e., for higher values of x. This behavior indicates an increase in CN_{Pb} or in the average Pb−O distances.[17] As lower NMR frequencies are associated with higher coordination numbers, the data in Figure 9 indicate a slight decrease in the average coordination of Pb when a small concentration of Al is added to the $Pb(PO_3)_2$ glass. This effect can be noticed directly on the spectrum of the $x = 0.08$ sample as an increase in the signal intensity in the region around −2000 ppm, with respect to the $x = 0$ sample. A further increase in the Al concentration causes a continuous increase in CN_{Pb}, well above the value corresponding to the $Pb(PO_3)_2$ glass.[15,16] Coordination numbers of this order were already observed in other phosphate glasses as Fe−Pb phosphate and Li−Na−Pb phosphate.[15,18] From these observations it can be concluded that Pb is acting as a modifier species in these glasses, across the entire compositional range.

The quantification of the Pb coordination number was attempted using a correlation between CN_{Pb} and the ^{207}Pb chemical shift, established from crystalline compounds.[17] According to these data, there is a shift of about −350 ppm for each O in the first coordination sphere of the Pb^{2+} ion. Hence, a linear relation between CN_{Pb} and the average ^{207}Pb chemical shift in these glasses can be defined using the value $CN_{Pb} = 8.4$ for the $Pb(PO_3)_2$ glass, which is the average of the measurements by EXAFS and X-ray diffraction.[15,16] The obtained values of CN_{Pb} vary within the range from 8.1 to 9.8, corresponding respectively to the glasses with $x = 0.15$ and $x = 0.73$.

Discussion

Phosphate Speciation. The populations of Q^2 and Q^2-(mAl) phosphate species and the coordination number of Al are useful quantities to understand how Pb and Al are preferentially bonded to NBO in the glass. Let us consider the number of phosphate tetrahedra with at least one NBO participating in the coordination sphere of one Al atom, N_{T-Al}. The total number of tetrahedra is

$$N_T = N_{T-Al} + N_{T-Pb} \quad (1)$$

where N_{T-Pb} is the number of tetrahedra with both NBO coordinated by Pb atoms. The quantity N_T/mol can be calculated for a certain glass composition as

$$N_T = 2 + x \quad (2)$$

To be able to calculate phosphate populations, it is necessary to introduce some information about Al bonding. Two hypotheses will be considered here, which will be subjected to the experimental test: (i) No Al−O−Al bridges are formed in the glass. (ii) Only one NBO from a phosphate tetrahedron will participate in the coordination sphere of an Al^{3+} ion; i.e., the glass network is formed by Q^2 and Q^2-(1Al).

Condition i will be straightforwardly satisfied in glasses with low Al concentration and no clustering. If this condition holds, the number N_{NBO-Al} of NBO linked to Al^{3+} ions will be

$$N_{NBO-Al} = xCN_{Al} \quad (3)$$

Condition ii was observed in Na−Al metaphosphate glasses,[23] where the linking of each Q^2 to two species (Na···O−P−O···Al) is the preferred bonding configuration for Al, compared with the linking only to Al (Al···O−P−O···Al), as long as the concentration of NBO is sufficiently high. The glass structure resulting from both conditions can be interpreted as a corner-sharing network of phosphate tetrahedra and AlO_n coordination polyhedra, favoring the mixing of chemical species linked to the NBO corners of PO_4 tetrahedra. If condition ii also holds in Pb−Al metaphosphate glasses, it is equivalent to write

$$N_{T-Al} = N_{NBO-Al} \quad (4)$$

If one combines (3) and (4), the number of Q^2(*1*Al) phosphates as a function of the Al concentration will be

$$N_{T-Al} = xCN_{Al} \quad (5)$$

Similarly, the number of Q^2 phosphates with no links to Al will be, if we combine (1) and (5),

$$N_{T-Pb} = 2 - x(CN_{Al} - 1) \quad (6)$$

The quantities given by eqs 5 and 6 may be compared with the relative fractions of Q^2 and Q^2(mAl) obtained by ^{31}P NMR. Figure 10 shows the experimental populations and the calculated ones under the assumptions i and ii, using eqs

(35) Van der Meer, H. *Acta Crystallogr.* **1976**, *B32*, 2423−2426.
(36) Shannon, R. D.; Prewitt, C. T. *Acta Crystallogr.* **1969**, *B25*, 925−946.
(37) Metwalli, E.; Brow, R. K. *J. Non-Cryst. Solids* **2001**, *289*, 113−122.

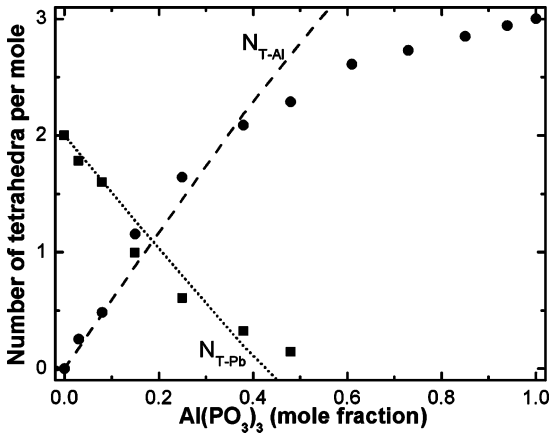

Figure 10. Number of Q^2 tetrahedral species/mol as a function of the composition: squares, Q^2 with no NBO linked to Al; circles, $Q^2(m\text{Al})$ with $m = 1$ or $m = 2$ NBO linked to Al; dashed line, calculation of N_{T-Al} from expression (5); dotted line, calculation of N_{T-Pb} from expression (6).

5 and 6 and the experimental $CN_{Al}(x)$. There is good agreement for glasses with $0 \leq x \leq 0.38$, indicating that the hypothesis assumed for the Al bonding is realistic in a significant concentration range. For glasses with $x > 0.38$, the calculated N_{T-Al} shows a substantial deviation with respect to the population of $Q^2(m\text{Al})$. The origin of this disagreement can be traced as a failure of condition ii for compositions richer in Al. Equation 6 is in itself valid just for glasses with x less than a certain critical concentration x_C, where $N_{T-Pb}(x_C) = 0$, establishing an absolute limit of applicability for condition ii. Using the observed CN_{Al} values, this concentration results as $x_C = 0.43 \pm 0.02$, corresponding to a network with all phosphates sharing one NBO with Al and the other with Pb. Therefore, a further increase in the Al content implies that $Q^2(2\text{Al})$ units should necessarly appear. The observation of some Q^2 for $x = 0.48$ suggests that the onset of $Q^2(2\text{Al})$ units occurs as a smooth process, beginning at concentrations slightly below the nominal limit $x_C = 0.43$.

Lead Coordination Environments. According to the evolution of the average ^{207}Pb chemical shift with the Al concentration, there is an increase in the coordination number around Pb. Some insight into this behavior, and on the degree of O-sharing between PbO_n polyhedra, can be gained by evaluating the ratio of [NBO/Pb]. As a starting point, only those NBOs not linked to Al will be accounted for

$$N_{NBO-Pb} = N_{NBO} - N_{NBO-Al} \tag{7}$$

where $N_{NBO} = 2(2 + x)$ is the total number of NBOs for a given composition. Equation 7 is equivalent to state that there are no Pb−O−Al bridges in the coordination sphere of Pb; i.e., there are no common corners between PbO_n and AlO_n coordination polyhedra. On the other hand, if condition i is assumed as valid for Al, the quantity N_{NBO-Al} can be readily calculated from eq 3. Therefore, the ratio $[N_{NBO-Pb}/Pb]$ can be written as

$$\left[\frac{N_{NBO-Pb}}{Pb}\right] = \frac{4 + x(2 - CN_{Al})}{1 - x} \tag{8}$$

The resulting values from eq 8, using the measured CN_{Al} as a function of x, are plotted in Figure 9. As can be seen, there is a remarkable correlation between the behavior of the average ^{207}Pb chemical shift and the $[N_{NBO-Pb}/Pb]$ ratio, with both quantities obtained from completely independent experiments. This result indicates that the observed shift of the ^{207}Pb spectra is governed by the relative availability of NBO as the Pb concentration is decreased, leading to Pb environments with progressively higher coordination number. The $Pb(PO_3)_3$ and, to a lesser degree, the $x = 0.08$ glasses lay slightly apart with respect to the general correlation, indicating structural differences with respect to the other compositions, as was also observed in the behavior of T_g and V_m. The correlation observed for glasses containing Al indicates that the two hypothesis leading to eq 8, namely the absence of NBO sharing between PbO_n and AlO_n polyhedra and between AlO_n polyhedra themselves, may accurately describe the average connectivity between these units and the phosphate groups. The calculated ratio $[N_{NBO-Pb}/Pb]$ increases from 4.0 to 5.6 between the compositions $x = 0$ and $x = 0.73$. These values are quite below 8, the coordination number for the lead metaphosphate glass, indicating a substantial sharing of NBO between PbO_n polyhedra. It can be estimated from these values that for glasses up to $x = 0.5$ each NBO is shared by two Pb atoms. This figure should increase for glasses richer in Al, but the estimation depends critically on a precise quantification of CN_{Pb}.

Conclusion

The incorporation of Al into the lead metaphosphate creates a stiffer and less packed glass network. The compositional dependence of several properties, as T_g, V_m, vibrational frequencies, and chemical shift, indicates a homogeneous dispersion of Al within the glass. Aluminum behaves as an intermediate species, establishing more covalent bonds as the concentration is increased. On the other hand, lead behaves as a modifier species for all compositions, establishing progressively more ionic bonds in Al-rich glasses. Increasingly higher Pb coordination numbers, above 8, are expected as Al is introduced into the glass. A tentative quantification indicates an increment in CN_{Pb} up to 9.8 for the glass with $x = 0.73$.

The analysis of the phosphate speciation in Pb−Al metaphosphate glasses shows definite short- and medium-range structural properties depending on the average way that AlO_n groups bind to phosphate tetrahedra. In glasses with $Al(PO_3)_3$ mole fraction less than 0.48, phosphate groups share preferentially only one NBO corner with an AlO_n coordination polyhedron. Above this concentration, more than one NBO can be linked to an AlO_n polyhedron. There is no appreciable degree of corner sharing among AlO_n and PbO_n polyhedra nor AlO_n themselves throughout the compositional range. In contrast, PbO_n coordination polyhedra show considerable NBO sharing, each oxygen participating in the coordination sphere of two Pb. This kind of medium

range organization, with AlO_n sharing corners only with PO_4, is consistent with the observation of less packed network as the Al concentration is increased. The bonding preferences determined for Al are in agreement with the behavior observed in Na−Al and Ca−Al metaphosphate glasses, indicating this may be a possible general trend for ternary phosphate glasses.

Acknowledgment. This research has financial support from FAPESP (Grant 07/61218-0) and CNPq (Grants 303116/2004-8 and 470526/2006-8). We wish to thank Prof. Edgar Zanotto for giving us access to his laboratory for glass preparation.

IC701707A